ELSEVIER

Journal of Alloys and Compounds 408–412 (2006) 140–143

Journal of ALLOYS AND COMPOUNDS

www.elsevier.com/locate/jallcom

Electronic configuration of Ce and Gd in $Ce_xGd_{1-x}N$ determined by XAFS (XANES and EXAFS) and magnetization measurements

H. Nitani [a,*], T. Nakagawa [a], T. Osuki [a], Y. Suzuki [a], M. Yamanouchi [a], T.A. Yamamoto [a], S. Emura [b]

[a] *Graduate School of Engineering, Osaka University, Suita, Osaka 565-0871, Japan*
[b] *The Institute of Scientific and Industrial Research, Osaka University, Ibaraki, Osaka 567-0047, Japan*

Available online 28 June 2005

Abstract

$Ce_xGd_{1-x}N$ were synthesized at various Ce atomic fractions x's and the electronic configurations of Ce and Gd were evaluated from the XANES measurement and the magnetization measurement. The obtained effective magnetic moment μ_{eff} was compared with the effective magnetic moment μ_{calc} calculated from the theoretical magnetization of Ce:$4f^0$, Ce:$4f^1$ and Gd:$4f^7$. Ce L_{III}-edge and Gd L_{III}-edge XANES spectra were compared with those of standard compounds. Both the results showed that Gd has [Xe]$4f^7$ electronic configuration, and Ce has the mixed configuration of [Xe]$4f^1$and [Xe]$4f^0$ when $x \leq 0.5$, and has [Xe]$4f^0$ configuration at higher x. The local structures around Ce and Gd elements were also determined by using EXAFS method and found that both of $R_{Ce–N}$ and $R_{Gd–N}$ increased with increasing x, and $R_{Ce–N}$ was always larger by an almost constant value than $R_{Gd–N}$ at any x.

Keywords: Binary rare earth nitride; XANES; EXAFS; Magnetization; Electronic states

1. Introduction

Rare earth compounds have been widely studied because of their potentialities for application to catalysts, magnetic materials, solid electrolytes and so on [1,2]. Ce is a typical multi-valence rare earth element. The valence of Ce varies from +4 to +3 with increasing temperature [3]. Gd has a large magnetic moment and a small magnetic anisotropy. GdN is a ferromagnetic material with the highest Curie temperature in the rare earth nitrides, and is an important component of the new magnetic materials [4]. The magnetic moment of an atom is caused by an angular momentum of electron. In a rare earth element, the magnetic moment reflects the states of 4f electrons, it is thus important to determine the configuration of 4f electrons of the rare earth elements in a compound for further improvement of new magnetic material. However, if the compound contains two or more rare earth elements, it is rather difficult to estimate the 4f electron state of each element through the unique magnetic measurements, because we can evaluate only the total contribution of the 4f electrons in the compound from the magnetic measurement. The X-ray absorption fine structure (XAFS) method is a useful technique to obtain the information on a chemical bonding such as electronic configuration, site symmetry and band structure for each element. XAFS consists of X-ray absorption near edge structure (XANES) and extended X-ray absorption fine structure (EXAFS). In the XANES method, the absorption coefficients of samples are measured within only a few tens electron volts around the absorption-edge energy. Since the absorption edge energy is inherent in each element, the XANES measurements were performed without interference of other elements [5]. The EXAFS reflects the atomic structure around the X-ray absorbing element. In this work, $Ce_xGd_{1-x}N$ samples at various mixing ratios were synthesized and the electronic configurations of Ce and Gd in $Ce_xGd_{1-x}N$ samples were evaluated by the XANES and magnetization measurements. The interatomic distances of Ce–N and Gd–N bonds were also determined by examining the local structures around Ce and Gd atoms by the EXAFS analysis.

* Corresponding author. Tel.: +81 6 6879 7887; fax: +81 6 6879 7887.
E-mail address: h-nitani@mit.eng.osaka-u.ac.jp (H. Nitani).

0925-8388/$ – see front matter © 2005 Elsevier B.V. All rights reserved.
doi:10.1016/j.jallcom.2005.04.067

2. Experimental

$Ce_xGd_{1-x}N$ samples were prepared according to carbothermic reduction. The appropriate amount of CeO_2 (99.99% purity) and Gd_2O_3 (99.99% purity) powders was mixed with carbon powder by using an agate mortar and a pestle. The atomic fraction, x, of Ce were chosen to be $x = 0.0$, 0.1, 0.3, 0.5, 0.7, 0.9 and 1.0. A little amount of polyvinyl alcohol was then added to the mixed powder as a binder. The sample was shaped into a pellet of 10 mm diameter and loaded on an alumina boat inserted into a reaction tube. The reaction tube was evacuated up to a vacuum of 10^{-5} Pa, and heated up to 1723 ± 2 K for 12 h to allow carbothermic reduction forming carbide. Then NH_3 gas (99.999% purity) was introduced into the reaction tube, and the temperature was adjusted to 1473 ± 2 K. The flow rate of NH_3 gas was kept at 200 ml/min for more than 5 h. Carbon remaining in the sample was removed as methane [6]. After this process, the samples were quenched down to room temperature. The obtained samples were analyzed by using XANES, magnetization and XRD measurements. Since the rare earth nitride is very sensitive to air or moisture, the sample was dispersed into a paraffin to avoid contact with air. The magnetization measurements were carried out with a superconducting quantum interference device (SQUID) magnetometer in the temperature range of 5–200 K under magnetic fields from 0 to 5 T. The XAFS measurements were performed at Ce L_{III}-edge (5723 eV) and Gd L_{III}-edge (7243 eV) on the BL-7C beam line of KEK-PF (High Energy Accelerator Research Organization, Japan). All the measurements were made in air at room temperature with the transmission mode, and two Si(1 1 1) crystals were used as a monochromator. The energy resolution was about 0.3 eV. The intensities of incident and transmitted X-rays were measured with ion chambers, which were filled with 100% N_2 gas for incident X-rays and with a mixture of 85% N_2 and 15% Ar gas for transmitted X-rays. The X-ray energy was calibrated at the Cu K-edge (8980 eV) of a Cu metal foil. To characterize the phase and lattice constant of samples, powder XRD measurements were performed by using RIGAKU RINT Ultima+ diffractometer with Cu Kα radiation.

3. Results and discussion

The magnetization of $Ce_xGd_{1-x}N$ obtained at 200 K is shown in Fig. 1 as a function of magnetic field. It is clear that the magnetization is proportional to magnetic field and the magnetization decreases with increasing atomic fraction x. This is because Ce of CeN has practically no electron on 4f orbital, that is, $[Xe]4f^0$ configuration. Fig. 2 shows a temperature dependence of magnetization of $Ce_{0.5}Gd_{0.5}N$, which indicates that $Ce_xGd_{1-x}N$ is a paramagnetic substance with the effective magnetic moment μ_{eff} depending on x. To evaluate μ_{eff}, these data-sets were fitted to the Currie–Weiss equation: $\chi = N\mu_{eff}^2/3k_B(T-\theta)$, where χ is the susceptibility M/H, N the number of magnetic atoms, k_B the Boltzmann constant, and θ is the asymptotic Curie point. μ_{eff} thus determined are plotted against x in Fig. 3. It shows that μ_{eff} decreases with increasing x and that the μ_{eff}'s of GdN ($x = 0$) and CeN ($x = 1$) agree with those calculated by assuming the electronic configurations of Gd:$[Xe]4f^7$ and Ce:$[Xe]4f^0$. These values are $\mu_{calc}(Gd{:}4f^7) = 7.94\mu_B/N_{Gd}$ and $\mu_{calc}(Ce{:}4f^0) = 0\mu_B/N_{Ce}$ which are calculated from to the Lande's g-formula, where μ_B is the Bohr magneton. When the atomic fraction of Ce is x, the effective magnetic moment of $Ce_xGd_{1-x}N$ is obtainable by the following formula:

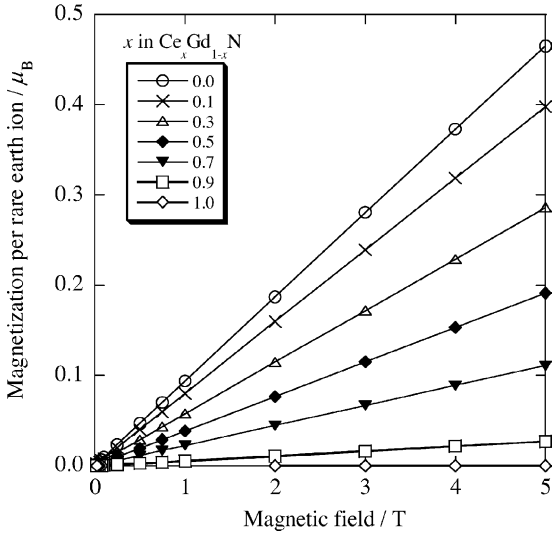

Fig. 1. Magnetization of $Ce_xGd_{1-x}N$ at 200 K at various magnetic fields.

$$\mu_{\text{eff-calc}} = \sqrt{x(\mu_{\text{calc}}(\text{Ce} : 4f^0))^2 + (1-x)(\mu_{\text{calc}}(\text{Gd} : 4f^7))^2} \quad (1)$$

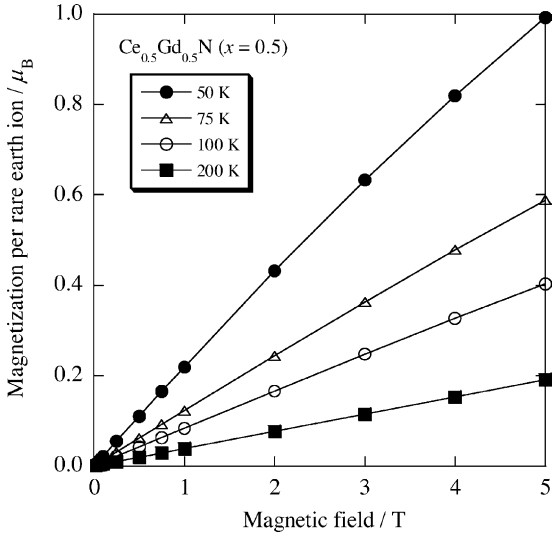

Fig. 2. Magnetization of $Ce_{0.5}Gd_{0.5}N$ measured at various temperatures and magnetic fields.

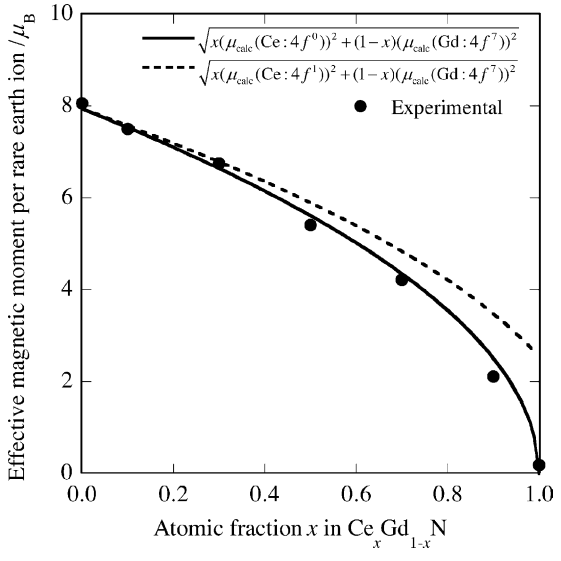

Fig. 3. Experimentally evaluated effective magnetic moments μ_{eff} of $Ce_xGd_{1-x}N$ and calculated effective magnetic moments μ_{calc}.

The values of μ_{eff} are described as the solid line in Fig. 3. The dashed line is the result when $\mu_{calc}(Ce{:}4f^1) = 2.54\mu_B/N_{Ce}$ in the above formula. The present experimental values seems to agree with the solid line, indicating that Gd and Ce have $[Xe]4f^7$ and $[Xe]4f^0$ configurations respectivery. However, the difference between the solid and the dashed curves for $x \leq 0.5$ is very small, both are indistinguishable.

The measured XANES spectra of (a) Ce L_{III}-edge and (b) Gd L_{III}-edge of $Ce_xGd_{1-x}N$ are depicted in Fig. 4 with that of CeF and GdF as reference substances which have $[Xe]4f^1$ and $[Xe]4f^7$ configurations, respectively. All the spectra were corrected for the background and normalized. The spectrum of Gd L_{III}-edge is substantially independent of atomic fraction x and agree with that of GdF_3. This result indicates that Gd of $Ce_xGd_{1-x}N$ has $[Xe]4f^7$ configuration for all the composition. However, there is a significant x-dependence on the spectrum of Ce L_{III}-edge. When $0.7 \leq x$, the spectrum of $Ce_xGd_{1-x}N$ have a double peak feature at 5727 and 5738 eV. This tendency is consistent with the spectrum of CeN. Thus, Ce should have $[Xe]4f^0$ configuration for $0.7 \leq x$. But when $x \leq 0.5$, the peak at 5727 eV is predominant. This feature is similar to that of CeF, which possess a single peak at 5727 eV. These six spectra are, therefore, divided into two sets, x = (0.1, 0.3, 0.5) and (0.7, 0.9, 1.0). The former has the mixed Ce configuration of $[Xe]4f^1$ and $[Xe]4f^0$, and the latter has only $[Xe]4f^0$ configuration.

As for EXAFS analyses, the backgrounds of XAFS spectra in the pre-edge and post edge regions were removed by a Victoreen function and a cubic spline function. Thus, background-removed EXAFS function $\chi(k)$ in the range $23 \leq k \leq 93\,nm^{-1}$ was Fourier transformed into the R-space to obtain the radial distribution function, RDF. The RDF was Fourier-back-transformed in the k-space by applying the Fourier filtering to the first peak of RDF, which results from the bonding between rare earth element and nitrogen. A curve fitting was performed with the EXAFS equation:

$$\chi(k) = \left(\frac{N}{kR^2}\right) F(k) e^{-2\sigma^2 k^2} e^{-2R/\lambda(k)} \sin(2kR + \phi(k)) \quad (2)$$

by using FEFFIT program [7]. In this equation, the backscattering amplitude $F(k)$, the phase shift $\phi(k)$ and the photoelectron's mean free path of photoelectron $\lambda(k)$ were calculated from the FEFF7 program assuming the single scattering path [8]. Optimized parameters in the fits were R, N, σ^2 and ΔE_0, where R is the interatomic distance, N the coordination number, σ^2 the Debye–Waller factor and ΔE_0 a correction to the edge-energy E_0. The values of the optimized parameters are

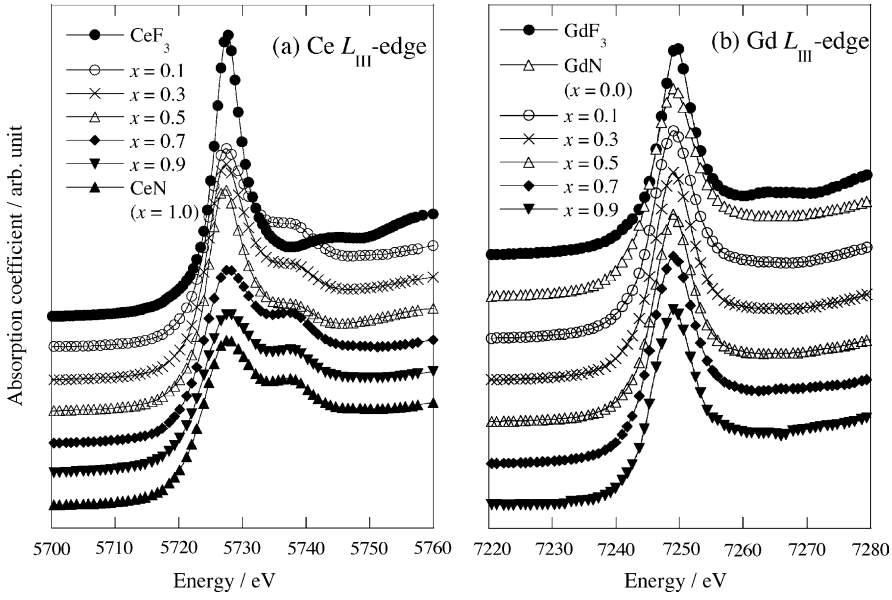

Fig. 4. XANES spectra of $Ce_xGd_{1-x}N$ samples (a) at Ce L_{III}-edge and (b) at Gd L_{III}-edge.

Table 1
Optimized parameters for Ce and Gd L_{III}-edge EXAFS analyses of $Ce_xGd_{1-x}N$

	Mixing ratio x	0.0	0.1	0.3	0.5	0.7	0.9	1.0
Ce L_{III}-edge	$R_{Ce–N}$ (nm)	–	–	0.2503	0.2504	0.2509	0.2512	0.2513
	σ^2 (10^{-5} nm^2)	–	–	9.84	6.60	19.66	16.45	11.98
	ΔE_0 (eV)	–	–	2.13	1.39	3.34	3.24	3.35
	R-factor[a]	–	–	0.0452	0.0572	0.0660	0.0570	0.0658
Gd L_{III}-edge	$R_{Gd–N}$ (nm)	0.2492	0.2486	0.2496	0.2498	0.2503	–	–
	σ^2 (10^{-5} nm^2)	6.91	7.59	5.85	6.06	6.02	–	–
	ΔE_0 (eV)	7.91	8.06	7.98	7.33	7.06	–	–
	R-factor[a]	0.0276	0.0208	0.0343	0.0325	0.1021	–	–

[a] R-factor is a measure for the precision of the fit (Ref. [9]).

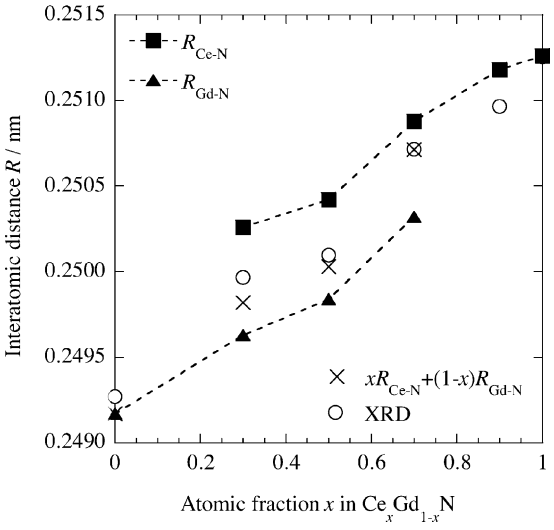

Fig. 5. Interatomic distances of Ce–N and Gd–N bonds evaluated by EXAFS and XRD.

given in Table 1 together with the R-factor which is a measure for the precision of the fit [9]. This R-factor is small enough to endorse the reliability of the present analysis. Evaluated interatomic distances, $R_{Ce–N}$ and $R_{Gd–N}$, are plotted in Fig. 5, which indicates that both the interatomic distances increase with increasing atomic fraction x, and that Gd attracts nitrogen nearer by about 0.0006 nm than Ce. In this figure, the average interatomic distances calculated as the linear combination of $xR_{Ce–N} + (1-x)R_{Gd–N}$ are as well plotted to be compared with the values estimated from the present XRD results. The present XRD results indicated that the metal sublattice obeys Vegard's law. In the ideal NaCl-type structure, metal-nitrogen distance is a half of the lattice parameter of fcc metal sublattice, so that it may be regarded as an average interatomic distance. It should be noticed that the average interatomic distances, which determined by two independent methods agree well with each other. This agreement would confirm the reliability of the present EXAFS analyses.

4. Conclusions

Binary rare earth nitride $Ce_xGd_{1-x}N$ was synthesized and the electronic configurations of Ce and Gd were evaluated from the XANES measurement and the magnetization measurement. The results obtained by the two independent techniques showed that the electronic configuration of Gd was $[Xe]4f^7$ for all composition, while that of Ce was the mixed configuration of $[Xe]4f^1$ and $[Xe]4f^0$ for low x and the single configuration of $[Xe]4f^0$ for high x. The interatomic distances $R_{Ce–N}$ and $R_{Gd–N}$ were determined by EXAFS analyses. The crystal structure is of NaCl-type in the whole range of x and the interatomic distance expands with increasing atomic fraction x.

References

[1] F. Hulliger, Handbook on the Physics and Chemistry of Rare Earths, vol. 4, Elsevier Science Publishers B.V., 1979.
[2] P. Wachter, E. Kaldis, Solid State Commun. 34 (1980) 241.
[3] R. Didchenko, F.P. Gortsema, J. Phys. Chem. Solids 24 (1963) 863.
[4] D.X. Li, Y. Haga, H. Shida, T. Suzuki, Physica B 199–200 (1994) 631.
[5] B.K. Teo, EXAFS: Basic Principles and Data Analysis, Springer-Verlag, Berlin, 1986, pp. 1–20.
[6] T. Nakagawa, H. Matsuoka, M. Sawa, K. Idehara, M. Miyake, M. Katsura, J. Nucl. Mater. 247 (1997) 147.
[7] M. Newville, B. Ravel, D. Haskel, J.J. Rehr, E.A. Stern, Y. Yacoby, Physica B 208–209 (1995) 154.
[8] S.I. Zabinsky, J.J. Rehr, A. Ankudinov, Phys. Rev. B 52 (1995) 2995.
[9] M. Newville, The Program Documentation of UWXAFS 3.0 Package: FEFFIT 2.32, The UWXAFS Project, University of Washington 1995, pp. 16–20.